Inorg. Chem. **2003**, *42*, 2004–2013

Amine-Templated Linear Vanadium Sulfates with Different Chain Structures

Geo Paul,[†] Amitava Choudhury,[†] R. Nagarajan,[‡] and C. N. R. Rao*,[†]

Chemistry and Physics of Materials Unit, Jawaharlal Nehru Centre for Advanced Scientific Research, Jakkur P.O., Bangalore 560 064, India, and Department of Condensed Matter Physics and Materials Science, Tata Institute of Fundamental Research, Mumbai 400 005, India

Received October 29, 2002

Amine-templated vanadium sulfates of the formula $[HN(CH_2)_6NH][(V^{IV}O)_2(OH)_2(SO_4)_2]\cdot H_2O$, **I**, $[H_3N(CH_2)_2NH_3][V^{III}(OH)(SO_4)_2]\cdot H_2O$, **II**, and $[H_2N(CH_2)_4NH_2][(V^{IV}O)(H_2O)(SO_4)_2]$, **III**, have been prepared under hydrothermal conditions. These vanadium sulfates add to the new emerging family of organically templated metal sulfates. Compound **I** has a linear chain structure consisting of V_2O_8 square-pyramid dimers connected by corner-sharing SO_4 tetrahedra, creating four-membered rings along the chain. Both **II** and **III** possess simple linear chain topologies formed by VO_6 octahedra and SO_4 tetrahedra, with **II** having the tancoite chain structure. Compound **I** crystallizes in the triclinic space group $P\bar{1}$ (No. 2) with $a = 7.4852(4)$ Å, $b = 9.5373(5)$ Å, $c = 11.9177(6)$ Å, $\alpha = 77.22°$, $\beta = 76.47(2)°$, $\gamma = 80.86°$, $Z = 2$. Compound **II**: monoclinic, space group $P2_1/c$ (No. 14), $a = 6.942(2)$ Å, $b = 10.317(3)$ Å, $c = 15.102(6)$ Å, $\beta = 90.64(4)°$, $Z = 4$. Compound **III**: triclinic, space group $P\bar{1}$ (No. 2) with $a = 6.2558(10)$ Å, $b = 7.0663(14)$ Å, $c = 15.592(4)$ Å, $\alpha = 90.46(2)°$, $\beta = 90.47(2)°$, $\gamma = 115.68(2)°$, $Z = 2$. Magnetic susceptibility measurements reveal weak antiferromagnetic interactions in **I** and **III** and ferromagnetic interactions in **II**.

Introduction

Although a variety of families of inorganic open-framework structures involving various anionic moieties such as silicates,[1] phosphates,[2] carboxylates,[3] and selenites[4] have been synthesized and described in the literature, open architectures formed by sulfates are relatively new. It is only recently that open-framework iron and cadmium sulfates have been reported.[5] One would expect open-framework transition metal sulfates to exhibit interesting magnetic properties as indeed revealed by the layered mixed-valent iron sulfates reported recently.[6] We have attempted to synthesize amine-templated vanadium sulfates by carrying out the reaction of V_2O_5 or $VOSO_4$ with an organic amine sulfate or with a mixture of an amine and sulfuric acid under hydrothermal conditions. By this means, we have obtained three organically templated linear-chain vanadium sulfates with the compositions $[HN(CH_2)_6NH][(V^{IV}O)_2(OH)_2(SO_4)_2]\cdot H_2O$, **I**, $[H_3N(CH_2)_2NH_3][V^{III}(OH)(SO_4)_2]\cdot H_2O$, **II**, and $[H_2N(CH_2)_4NH_2][(V^{IV}O)(H_2O)(SO_4)_2]$, **III**. In **I**, the linear chain is formed by dimers of vanadium−oxygen square-pyramids connected by two SO_4 units, so as to give rise to corner-shared four-membered rings, while **II** and **III** contain simple chains formed by vanadium octahedra and sulfate tetrahedra.

Experimental Section

Synthesis and Initial Characterization. Compounds **I**−**III** were synthesized by employing mild hydro/solvothermal methods. The organic amines employed in **I**, **II**, and **III** are 1,4-diazabicyclo-

* To whom correspondence should be addressed. E-mail: cnrrao@jncasr.ac.in. Fax: +91-80-8462766.
† Jawaharlal Nehru Centre for Advanced Scientific Research.
‡ Tata Institute of Fundamental Research.

(1) (a) Breck, D. W. *Zeolite Molecular Sieves*; Wiley: New York, 1974. (b) Meier, W. M.; Oslen, D. H.; Baerlocher, C. *Atlas of Zeolite Structure Types*; Elsevier: London, 1996.
(2) (a) Cheetham, A. K.; Férey, G.; Loiseau, T. *Angew. Chem., Int. Ed.* **1999**, *38*, 3268. (b) Rao, C. N. R.; Natarajan, S.; Choudhury, A.; Neeraj, S.; Ayi, A. A. *Acc. Chem. Res.* **2001**, *34*, 80.
(3) (a) Serpaggi, F.; Ferey, G. *J. Mater. Chem.* **1998**, *8*, 2737. (b) Vaidhyanathan, R.; Natarajan, S.; Rao, C. N. R. *Chem. Mater.* **2001**, *13*, 185 and references therein.
(4) (a) Choudhury, A.; Udayakumar D.; Rao, C. N. R. *Angew. Chem., Int. Ed.* **2002**, *41*, 158 and references therein. (b) Harrison, W. T. A.; Phillips, M. L. F.; Stanchfield, J.; Nenoff, T. M. *Angew. Chem., Int. Ed.* **2000**, *39*, 3808.
(5) (a) Choudhury, A.; Krishnamoorthy, J.; Rao, C. N. R. *Chem. Commun.* **2001**, 2610. (b) Paul, G.; Choudhury, A.; Rao, C. N. R. *J. Chem. Soc., Dalton Trans.* **2002**, 3859. (c) Paul, G.; Choudhury, A.; Rao, C. N. R. *Chem. Commun.* **2002**, 1904.
(6) Paul, G.; Choudhury, A.; Sampathkumaran, E. V.; Rao, C. N. R. *Angew. Chem., Int. Ed.* **2002**, *41*, 4297.

10.1021/ic020645v CCC: $25.00
Published on Web 02/26/2003

Table 1. Synthetic Conditions and Analysis for Compounds **I**−**III**

	starting composition[a]	T (K)	t (h)	pH[b]	V/S[c]	formula	yield %[d]
I	2 V_2O_5:3 DABCOS[e]:50 buta-2-nol:50 H_2O	453	144	2 (3)	1/1	$[HN(CH_2)_6NH][(V^{IV}O)_2(OH)_2(SO_4)_2]\cdot H_2O$	60
II	3 $VOSO_4\cdot 5H_2O$:1 en:2 H_2SO_4[f]:50 EG[g]	453	48	2 (2)	1/2	$[H_3N(CH_2)_2NH_3][V^{III}(OH)(SO_4)_2]\cdot H_2O$	45
III	$VOSO_4\cdot 5H_2O$:3 PIPS[h]:50 H_2O	453	48	2 (2)	1/2	$[H_2N(CH_2)_4NH_2][(V^{IV}O)(H_2O)(SO_4)_2]$	50

[a] The absolute quantities of vanadium source taken are 0.1091 g for **I**, 0.7900 g for **II**, and 0.2531 g for **III**. [b] The value in the parentheses indicates the final pH. [c] The ratios of the heavy elements were obtained from EDX. [d] The yields were calculated with respect to vanadium. [e] 1,4-Diazabicyclo[222]octane sulfate. [f] The H_2SO_4 used was 98% (w/w) in water. [g] Ethylene glycol. [h] Piperazinium sulfate.

[222]octane (DABCO), ethylenediamine (en), and piperazine (PIP), respectively. Compounds **I** and **III** were prepared by employing the organoammonium sulfate as the source of the sulfate and the amine. Piperazine sulfate, $[H_2N(CH_2)_4NH_2](SO_4)\cdot H_2O$ (PIPS), and 1,4-diazabicyclo[222]octane sulfate, $[HN(CH_2)_6NH](SO_4)$ (DABCOS), were prepared following the procedures reported in the literature.[7] In a typical synthesis, as in the case of **I**, 0.1091 g of V_2O_5 was dispersed in a 2-butanol/H_2O mixture (1.4 mL/0.27 mL) under constant stirring. To this mixture was added 0.1892 g of DABCOS and the mixture stirred for 30 min. The final mixture with the molar composition 2 V_2O_5/3 DABCOS/50 butan-2-ol/50 H_2O was transferred into a 7 mL PTFE-lined acid digestion bomb and heated at 180 °C for 6 days. The product contained deep blue rhombohedral crystals and was monophasic (yield 60%). Details of the synthetic conditions for the preparation of the various vanadium sulfates are listed in Table 1. Compounds **I**−**III** were characterized by powder X-ray diffraction (XRD), thermogravimetric analysis (TGA), energy dispersive X-ray analysis (EDX), elemental CHN analysis, and IR spectroscopy. Magnetic measurements on powdered samples were performed at temperatures between 4 and 300 K, with a field of 200 and 5000 Oe, using a Quantum Design SQUID magnetometer.

All the three vanadium sulfates gave satisfactory elemental analysis. The experimental and calculated (in wt %) values for C, H, and N are as follows: **I**, C, 14.48; N, 5.38; H, 4.06; (calcd: C, 14.74; N, 5.73; H, 3.68); **II**, C, 6.97; N, 8.18; H, 3.54; (calcd: C, 7.06; N, 8.23; H, 3.82); **III**, C, 12.96; N, 6.94; H, 3.83 (calcd: C, 13.14; N, 7.67; H, 4.79).

The IR spectra of **I** and **III** exhibit, in addition to the amine bands, strong bands in the 960−980 cm^{-1} region due to ν(V═O). This band is absent in **II**. The spectra of **I**−**III** show multiple strong bands in the 1000−1040 cm^{-1} region due to ν_1 and in the 1050−1200 region due to ν_3 of the sulfate group.[8] The bending modes of SO_4^{2-} are found in the 400−500 and 600−700 cm^{-1} regions. The bands at 806 and 606 cm^{-1} in **I** are assigned to the stretching modes of the VO_5 group. Apart from the broad bands due to ν(O−H) and ν(N−H) in the 3200−3500 cm^{-1} region, a strong band is observed around 1020−1040 cm^{-1} in **I** and **II** due to the V−O−H bending mode. The band at 880 cm^{-1} in **III** is likely to be due to coordinated water.

Single-Crystal Structure Determination. Suitable single crystals of all the three compounds were carefully selected under a polarizing microscope and glued to a thin glass fiber with cyanoacrylate (superglue) adhesive. Single-crystal data were collected on a Siemens SMART-CCD diffractometer [graphite-monochromated Mo Kα radiation, $\lambda = 0.71073$ Å ($T = 298$ K)]. An absorption correction based on symmetry-equivalent reflections was applied using SADABS.[9] The structures were solved by direct methods using SHELXS-86[10] and difference Fourier synthesis. The direct methods solution readily revealed the heavy atom position (V and S) and enabled us to locate the other non-hydrogen positions (O, C, and N) from the Fourier difference maps. Hydrogen positions for the bonded [O(2) and O(3) in **I**, O(9) in **II,** and O(3) in **III**] as well as the extra-framework amine molecules [**I** and **III**] and water molecule [O(100) in **II**] were located from the difference Fourier map, placed in the observed position, and refined isotropically. All the hydrogen positions for the amine molecule in **II** were initially located in the difference Fourier maps, and for the final refinement, the hydrogen atoms were placed geometrically and held in the riding mode. The last cycles of refinement included atomic positions for all the atoms, anisotropic thermal parameters for all non-hydrogen atoms, and isotropic thermal parameters for all the hydrogen atoms. However, hydrogens for the extra-framework water molecule in **I** have not been included in the final refinement due to disorder that site (O20 with SOF = 0.65 and O20A with SOF = 0.35). Full-matrix least-squares structure refinement against $|F^2|$ was carried out using the SHELXTL-PLUS[11] package of programs. Details of the final refinements are given in Table 2. The powder X-ray diffraction patterns of all the three compounds were in good agreement with the simulated patterns generated from the single-crystal XRD data. Selected values of the bond distances and bond angles for **I**−**III** are listed in Tables 3−5, respectively. Various hydrogen bond interactions in **I**−**III** are listed in Table 6.

Table 2. Crystal Data and Structure Refinement Parameters for **I**−**III**

structural param	**I**	**II**	**III**
empirical formula	$[C_6N_2H_{14}][(V^{IV}O)_2(OH)_2(SO_4)_2]\cdot H_2O$	$[C_2N_2H_{10}][V^{III}(OH)(SO_4)_2]\cdot H_2O$	$[C_4N_2H_{12}][(V^{IV}O)(H_2O)(SO_4)_2]$
fw	490.21	340.20	365.23
space group	$P\bar{1}$	$P2_1/c$	$P\bar{1}$
a, Å	7.4852(4)	6.942(2)	6.2558(10)
b, Å	9.5373(5)	10.317(3)	7.0663(14)
c, Å	11.9177(6)	15.102(6)	15.592(4)
α, deg	77.22	90	90.46(2)
β, deg	76.470(2)	90.64(4)	90.47(2)
γ, deg	80.86(2)	90	115.68(2)
V, Å^3	801.52(7)	1081.6(6)	621.1(2)
Z	2	4	2
T, °C	20	20	20
λ(Mo Kα), Å	0.71073	0.71073	0.71073
θ range, deg	1.79−23.25	2.39−23.27	1.31−23.29
ρ_{calcd}, g cm^{-3}	2.031	2.089	1.953
μ, mm^{-1}	1.498	1.353	1.186
R1[a]	0.0488	0.0780	0.0318
wR2[b]	0.0931	0.1600	0.0753

[a] $R1 = \sum||F_o| - |F_c||/\sum|F_o|$. [b] $wR2 = \{\sum[w(F_o^2 - F_c^2)^2]/\sum[w(F_o^2)^2]\}^{1/2}$, $w = 1/[\sigma^2(F_o)^2 + (aP)^2 + bP]$, $P = [F_o^2 + 2F_c^2]/3$; where $a = 0.0439$ and $b = 0.9298$ for **I**, $a = 0.0424$ and $b = 12.4150$ for **II**, $a = 0.0399$ and $b = 0.4644$ for **III**.

(7) Krishnamoorthy, J.; Choudhury, A.; Rao, C. N. R. *Solid State Sci.* **2002**, *4*, 413.

(8) (a) Selbin, J.; Holmes, L. H.; McGlynn, S. P. *J. Inorg. Nucl. Chem.* **1963**, *25*, 1359. (b) Nakamoto, K. *Infrared and Raman Spectra of Inorganic and Coordination Compounds*; Wiley: NewYork, 1978.

(9) Sheldrick, G. M. *SADABS: Siemens Area Detector Absorption Correction Program*; University of Göttingen: Göttingen, Germany, 1994.

(10) (a) Sheldrick, G. M. *SHELXS-86: Program for crystal structure determination*; University of Göttingen: Göttingen, Germany, 1986. (b) Sheldrick, G. M. *Acta Crystallogr., Sect A.* **1990**, *35*, 467.

(11) Sheldrick, G. M. *SHELXTL-PLUS Program for Crystal Structure Solution and Refinement*; University of Göttingen: Göttingen, Germany.

Table 3. Selected Bond Distances and Angles in $[HN(CH_2)_6NH][(V^{IV}O)_2(OH)_2(SO_4)_2]\cdot H_2O$, **I**[a]

moiety	distance (Å)	moiety	angle (deg)	moiety	angle (deg)
V(1)−O(1)	1.580(3)	O(1)−V(1)−O(2)	111.4(2)	O(7)$^{\#2}$−V(2)−O(8)	92.69(11)
V(1)−O(2)	1.932(3)	O(1)−V(1)−O(3)	107.2(2)	O(9)−S(1)−O(10)	113.2(2)
V(1)−O(3)	1.952(3)	O(2)−V(1)−O(3)	75.27(14)	O(9)−S(1)−O(7)	108.2(2)
V(1)−O(4)$^{\#1}$	1.999(3)	O(1)−V(1)−O(4)$^{\#1}$	102.11(14)	O(10)−S(1)−O(7)	111.8(2)
V(1)−O(5)	2.008(3)	O(2)−V(1)−O(4)$^{\#1}$	87.71(12)	O(9)−S(1)−O(5)	109.5(2)
V(2)−O(6)	1.586(3)	O(3)−V(1)−O(4)$^{\#1}$	149.89(14)	O(10)−S(1)−O(5)	108.0(2)
V(2)−O(3)	1.944(3)	O(1)−V(1)−O(5)	100.46(14)	O(7)−S(1)−O(5)	105.7(2)
V(2)−O(2)	1.959(3)	O(2)−V(1)−O(5)	147.32(13)	O(11)−S(2)−O(12)	112.8(2)
V(2)−O(7)$^{\#2}$	2.002(3)	O(3)−V(1)−O(5)	89.05(12)	O(11)−S(2)−O(8)	109.8(2)
V(2)−O(8)	2.008(3)	O(4)$^{\#1}$−V(1)−O(5)	92.53(11)	O(12)−S(2)−O(8)	108.6(2)
S(1)−O(9)	1.441(3)	O(6)−V(2)-O(3)	108.7(2)	O(11)−S(2)−O(4)	108.3(2)
S(1)−O(10)	1.448(3)	O(6)−V(2)-O(2)	105.9(2)	O(12)−S(2)−O(4)	111.8(2)
S(1)−O(7)	1.498(3)	O(3)−V(2)-O(2)	74.83(14)	O(8)−S(2)−O(4)	105.3(2)
S(1)−O(5)	1.500(3)	O(6)−V(2)-O(7)$^{\#2}$	101.60(14)	V(1)−O(2)−V(2)	105.0(2)
S(2)−O(11)	1.447(3)	O(3)−V(2)-O(7)$^{\#2}$	88.59(13)	V(2)−O(3)−V(1)	104.9(2)
S(2)−O(12)	1.455(3)	O(2)−V(2)-O(7)$^{\#2}$	151.26(13)	S(2)−O(4)−V(1)$^{\#2}$	134.1(2)
S(2)−O(8)	1.501(3)	O(6)−V(2)-O(8)	102.04(14)	S(1)−O(5)−V(1)	121.9(2)
S(2)−O(4)	1.501(3)	O(3)−V(2)-O(8)	148.29(14)	S(1)−O(7)−V(2)$^{\#1}$	136.3(2)
		O(2)−V(2)−O(8)	89.75(12)	S(2)−O(8)−V(2)	119.1(2)

[a] Symmetry transformations used to generate equivalent atoms: #1, $x + 1$, y, z; #2, $x - 1$, y, z.

Table 4. Selected Bond Distances and Angles in $[H_3N(CH_2)_2NH_3][V^{III}(OH)(SO_4)_2]\cdot H_2O$, **II**[a]

moiety	distance (Å)	moiety	angle (deg)	moiety	angle (deg)
S(1)−O(1)	1.431(7)	O(1)−S(1)−O(2)	111.3(5)	O(4)−V(1)-O(8)$^{\#2}$	88.6(2)
S(1)−O(2)	1.461(7)	O(1)−S(1)−O(3)	111.5(4)	O(9)$^{\#1}$−V(1)−O(8)$^{\#3}$	88.1(2)
S(1)−O(3)	1.475(6)	O(2)−S(1)−O(3)	110.5(4)	O(9)−V(1)-O(8)$^{\#3}$	91.9(2)
S(1)−O(4)	1.508(6)	O(1)−S(1)−O(4)	107.8(4)	O(4)$^{\#1}$−V(1)−O(8)$^{\#3}$	88.6(2)
S(2)−O(5)	1.427(7)	O(2)−S(1)−O(4)	106.4(4)	O(4)−V(1)-O(8)$^{\#3}$	91.4(2)
S(2)−O(6)	1.453(6)	O(3)−S(1)−O(4)	109.2(3)	O(8)$^{\#2}$−V(1)−O(8)$^{\#3}$	180
S(2)−O(7)	1.500(6)	O(5)−S(2)−O(6)	112.4(4)	O(9)−V(2)-O(9)$^{\#3}$	180
S(2)−O(8)	1.501(6)	O(5)−S(2)−O(7)	108.8(4)	O(9)−V(2)-O(7)$^{\#3}$	88.8(2)
V(1)−O(9)$^{\#1}$	1.960(5)	O(6)−S(2)−O(7)	108.6(4)	O(9)$^{\#3}$−V(2)−O(7)$^{\#3}$	91.2(2)
V(2)−O(3)$^{\#3}$	2.053(5)	O(5)−S(2)−O(8)	109.8(4)	O(9)−V(2)−O(7)	91.2(2)
V(1)−O(4)$^{\#1}$	2.022(6)	O(6)−S(2)−O(8)	109.4(3)	O(9)$^{\#3}$−V(2)−O(7)	88.8(2)
V(1)−O(8)$^{\#2}$	2.055(5)	O(7)−S(2)−O(8)	107.6(3)	O(7)$^{\#3}$−V(2)−O(7)	180
V(2)−O(9)$^{\#3}$	1.964(5)	O(9)$^{\#1}$−V(1)−O(9)	180	O(9)−V(2)−O(3)#3	87.6(2)
V(2)−O(7)$^{\#3}$	2.016(6)	S(2)−O(7)−V(2)	132.2(3)	O(9)$^{\#3}$−V(2)−O(3)$^{\#3}$	92.4(2)
		S(2)−O(8)−V(1)$^{\#4}$	132.6(3)	O(7)$^{\#3}$−V(2)−O(3)$^{\#3}$	88.3(2)
		V(1)−O(9)−V(2)	124.4(3)	O(7)−V(2)−O(3)$^{\#3}$	91.7(2)
		O(9)$^{\#1}$−V(1)−O(4)$^{\#1}$	88.7(2)	O(9)−V(2)−O(3)	92.4(2)
		O(9)−V(1)-O(4)$^{\#1}$	91.3(2)	O(9)$^{\#3}$−V(2)−O(3)	87.6(2)
		O(9)$^{\#1}$−V(1)−O(4)	91.3(2)	O(7)$^{\#3}$−V(2)−O(3)	91.7(2)
		O(9)−V(1)-O(4)	88.7(2)	O(7)−V(2)−O(3)	88.3(2)
		O(4)$^{\#1}$−V(1)−O(4)	180	O(3)$^{\#3}$−V(2)−O(3)	180
		O(9)$^{\#1}$−V(1)−O(8)$^{\#2}$	91.9(2)	S(1)−O(3)−V(2)	134.3(3)
		O(9)−V(1)-O(8)$^{\#2}$	88.1(2)	S(1)−O(4)−V(1)	130.4(3)
		O(4)$^{\#1}$−V(1)−O(8)$^{\#2}$	91.4(2)		

[a] Symmetry transformations used to generate equivalent atoms: #1, $-x + 1$, $-y$, $-z$; #2, $x + 1$, y, z; #3, $-x$, $-y$, $-z$; #4, $x - 1$, y, z.

Results

$[HN(CH_2)_6NH][(V^{IV}O)_2(OH)_2(SO_4)_2]\cdot H_2O$, I. The asymmetric unit of **I** (Figure 1a) contains 25 non-hydrogen atoms of which 16 belong to the inorganic framework with 2 crystallographically distinct vanadium atoms and 2 sulfur atoms, and 8 belong to the amine molecule besides the presence of extra-framework water molecules. The five coordinated vanadium sites [V(1) and V(2)] exhibit the square-pyramidal geometry with the basal positions defined by the oxygen donors from each of the two adjacent sulfate groups and two hydroxyl donors and the apical position by the terminal oxide group. Each square-pyramid forms two (V−O−S) bonds, two (V−(OH)−V) bonds, and one V═O apical bond. Each tetrahedron forms two (S−O−V) bonds and the remaining two are terminal S═O bonds. The $VO_3(OH)_2$ square-pyramids and SO_4 tetrahedra constitute the 1D chain in **I**. The $V(1)O_3(OH)_2$ and $V(2)O_3(OH)_2$ pyramids share a common edge via two hydroxyl oxygens, with their apices on the opposite sides of the basal plane, to form V_2O_8 dimers. These V_2O_8 dimers are bridged by the sulfate tetrahedra on either side via corner sharing to form four-member rings that propagate along the *a*-axis (Figure 1b).

The basal V−O bond distances are in the range 1.932(2)−2.009(3) Å [$(V(1)-O)_{av} = 1.973(3)$ Å and $(V(2)-O)_{av} = 1.978(3)$ Å]. The apical V═O bond distances are 1.581(3) and 1.585(3) Å for V(1) and V(2), respectively. These V═O bond lengths are comparable to those observed in $VOSO_4\cdot 5H_2O$ (1.591 Å) but shorter than those in anhydrous $VOSO_4$ (1.630 Å).[12] The tetrahedral S−O bond distances are in the range 1.442(3)−1.501(3) Å [$(S(1)-O)_{av} = 1.472(3)$ Å and $(S(2)-O)_{av} = 1.475(3)$ Å], with the longest one

(12) (a) Ballhausen, C. J.; Djurinskji, B. F.; Watson, K. J. *J. Am. Chem. Soc*. **1968**, *90*, 3305. (b) Longo, J. M.; Arnott, R. J. *J. Solid State Chem*. **1970**, *1*, 394 and references therein.

Table 5. Selected Bond Distances and Angles in $[H_2N(CH_2)_4NH_2][(V^{IV}O)(H_2O)(SO_4)_2]$, **III**[a]

moiety	distance (Å)	moiety	angle (deg)	moiety	angle (deg)
V(1)−O(1)	1.582(2)	O(1)−V(1)−O(2)	101.94(10)	O(7)−S(1)−O(8)	111.64(14)
V(1)−O(2)	1.996(2)	O(1)−V(1)−O(3)	105.22(12)	O(7)−S(1)−O(6)	109.83(13)
V(1)−O(3)	1.997(3)	O(2)−V(1)−O(3)	85.52(11)	O(8)−S(1)−O(5)	110.39(13)
V(1)−O(4)	2.005(2)	O(1)−V(1)−O(4)	100.81(10)	O(6)−S(1)−O(5)	103.43(12)
V(1)−O(5)	2.046(2)	O(2)−V(1)−O(4)	157.06(8)	O(7)−S(1)−V(1)	126.59(10)
V(1)−O(6)	2.351(2)	O(3)−V(1)−O(4)	85.72(11)	O(8)−S(1)−V(1)	121.45(10)
S(1)−O(7)	1.452(2)	O(1)−V(1)−O(5)	98.00(10)	O(6)−S(1)−V(1)	57.62(8)
S(1)−O(8)	1.457(2)	O(2)−V(1)−O(5)	90.79(9)	O(5)−S(1)−V(1)	45.90(8)
S(1)−O(6)	1.489(2)	O(3)−V(1)−O(5)	156.76(11)	O(10)−S(2)−O(9)	113.0(2)
S(1)−O(5)	1.500(2)	O(4)−V(1)−O(5)	88.96(9)	O(10)−S(2)−O(2)$^{\#1}$	110.03(14)
S(2)−O(10)	1.434(2)	O(1)−V(1)−O(6)	162.07(10)	O(9)−S(2)−O(2)$^{\#1}$	110.51(14)
S(2)−O(9)	1.436(2)	O(2)−V(1)−O(6)	79.10(8)	O(10)−S(2)−O(4)	109.67(14)
S(2)−O(2)$^{\#1}$	1.492(2)	O(3)−V(1)−O(6)	92.72(10)	O(9)−S(2)−O(4)	110.64(14)
S(2)−O(4)	1.502(2)	O(4)−V(1)−O(6)	80.19(8)	O(2)$^{\#1}$−S(2)−O(4)	102.54(11)
		O(5)−V(1)−O(6)	64.07(8)	S(2)$^{\#2}$−O(2)−V(1)	131.91(13)
		O(1)−V(1)−S(1)	129.75(9)	V(1)−O(3)−H(13)	125(4)
		O(2)−V(1)−S(1)	85.31(7)	V(1)−O(3)−H(14)	127(4)
		O(3)−V(1)−S(1)	124.99(9)	H(13)−O(3)−H(14)	108(5)
		O(4)−V(1)−S(1)	82.45(6)	S(2)−O(4)−V(1)	127.75(12)
		O(5)−V(1)−S(1)	31.77(6)	S(1)−O(5)−V(1)	102.33(11)
		O(6)−V(1)−S(1)	32.34(5)	S(1)−O(6)−V(1)	90.04(9)

[a] Symmetry transformations used to generate equivalent atoms: #1, $x + 1$, y, z; #2, $x - 1$, y, z.

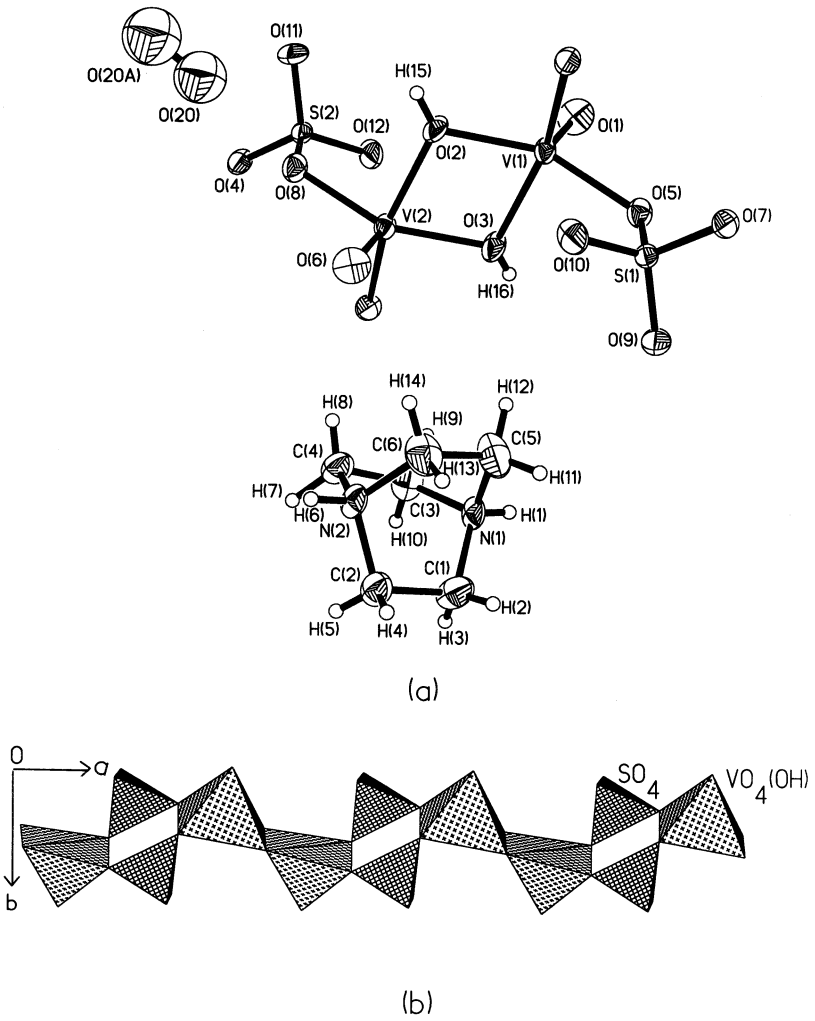

Figure 1. (a) ORTEP plot of $[HN(CH_2)_6NH][(V^{IV}O)_2(OH)_2(SO_4)_2]\cdot H_2O$, **I**. The asymmetric unit is labeled. Thermal ellipsoids are given at 50% probability. (b) Polyhedral view of the inorganic part of **I**, showing the vanadium square-pyramid dimers bridged by sulfate tetrahedra to form four-membered rings.

involving the oxygen atom coordinated to the vanadium center. The V−(μ-O)−(H) distance in the [V−(μ_2-OH)$_2$−V] is in the range 1.932(3)−1.959(3) Å, comparable to that of similar bonds reported earlier, but significantly different from the V−(μ-O) and V−(μ-O)(H$_2$) lengths in the literature.[13] The V−O distance along with the results of the bond valence sum (BVS) calculations[14] and the observed electron density near the oxygens [O(2) and O(3)] in the difference

Table 6. Hydrogen Bonding Interactions in Compounds **I**−**III**

D−H···A	D−H (Å)	H···A (Å)	D···A (Å)	D−H···A (deg)
		I		
N(1)−H(1)···O(5)	0.77(5)	2.12(5)	2.808(5)	148(5)
N(2)−H(6)···O(8)	0.84(5)	2.34(4)	2.985(5)	134(4)
N(2)−H(6)···O(10)	0.84(5)	2.09(5)	2.761(5)	137(4)
O(2)−H(15)···O(11)	0.71(4)	2.06(4)	2.744(4)	163(5)
O(3)−H(16)···O(9)	0.64(5)	2.11(5)	2.724(5)	159(6)
C(2)−H(4)···O(11)	0.94(5)	2.49(5)	3.358(6)	154(4)
C(2)−H(5)···O(20)	0.89(5)	2.52(5)	3.283(10)	144(4)
C(4)−H(7)···O(20)	1.00(5)	2.39(5)	3.185(10)	135(4)
		II		
N(1)−H(1)···O(7)	0.889(10)	2.069(9)	2.919(9)	159.4(8)
N(1)−H(2)···O(1)	0.891(11)	1.890(10)	2.760(10)	164.7(8)
N(1)−H(3)···O(6)	0.890(10)	2.103(9)	2.961(9)	161.6(8)
N(2)−H(9)···O(2)	0.891(11)	2.362(10)	3.017(10)	130.4(8)
N(2)−H(10)···O(6)	0.890(11)	2.168(11)	2.961(11)	148.1(8)
N(2)−H(10)···O(7)	0.890(11)	2.525(10)	3.331(10)	150.9(8)
O(100)−H(11)···O(1)	1.00(13)	2.29(12)	3.186(11)	149(12)
O(100)−H(11)···O(2)	1.00(13)	2.21(15)	3.080(10)	145(13)
O(100)−H(12)···O(5)	1.00(8)	2.20(9)	2.958(10)	132(6)
O(9)−H(13)···O(100)	0.96(11)	1.75(11)	2.695(10)	168(10)
		III		
N(1)−H(1)···O(4)	0.79(4)	2.45(3)	3.020(4)	131(3)
N(1)−H(1)···O(8)	0.79(4)	2.46(4)	3.072(4)	136(3)
N(1)−H(2)···O(6)	0.86(4)	2.21(5)	3.011(5)	154(3)
N(1)−H(2)···O(7)	0.86(4)	2.38(4)	3.095(4)	140(3)
N(2)−H(7)···O(10)	0.86(4)	1.91(4)	2.735(4)	160(3)
N(2)−H(8)···O(9)	0.83(4)	2.00(4)	2.761(4)	154(4)
O(3)−H(13)···O(7)	0.70(5)	1.99(5)	2.670(4)	166(5)
O(3)−H(14)···O(8)	0.77(6)	1.93(6)	2.679(4)	165(6)

Fourier map help to identify O(2) and O(3) as belonging to hydroxyl groups. BVS calculations [V(1) = 4.14 and V(2) = 4.08] also indicate the valence state of vanadium to be +4. The chains in **I** are interconnected via hydrogen bonds [N−H···O, O−H···O, and C−H···O] formed by the diprotonated amine molecules and the extra-framework water molecules as shown in Figure 2a. The 3D assembly shown in Figure 2b is formed by the inorganic chains and the diprotonated amine molecules along with the extraframework water molecules. Selected values of the bond distances and angles in **I** are listed in Table 3 and the various hydrogen bond interactions in Table 6.

$[H_3N(CH_2)_2NH_3][V^{III}(OH)(SO_4)_2]\cdot H_2O$, II. The asymmetric unit of **II** consists of 18 non-hydrogen atoms with 2 crystallographically distinct V and S atoms as shown in Figure 3a. The structure is built up from 13 framework atoms containing $VO_4(OH)_2$ octahedra and SO_4 tetrahedra. The V atoms make four V−O−S links and two V−(OH)−V links to the neighboring S atoms and V atoms, respectively. Similarly, the S atoms form two S−O−V bonds with each of the adjacent vanadium atoms, the remaining two being S═O terminal bonds. The framework structure is built up of isolated infinite chains of $[V(OH)(SO_4)_2]^{2-}{}_n$ running along the *a*-axis. In the $[V(OH)(SO_4)_2]^{2-}{}_n$ chain, the $VO_4(OH)_2$ octahedra share vertices in a trans fashion via the (OH) groups, and the SO_4 tetrahedra are grafted on to the chain in a symmetrical bridge. The trans orientation of the bridging

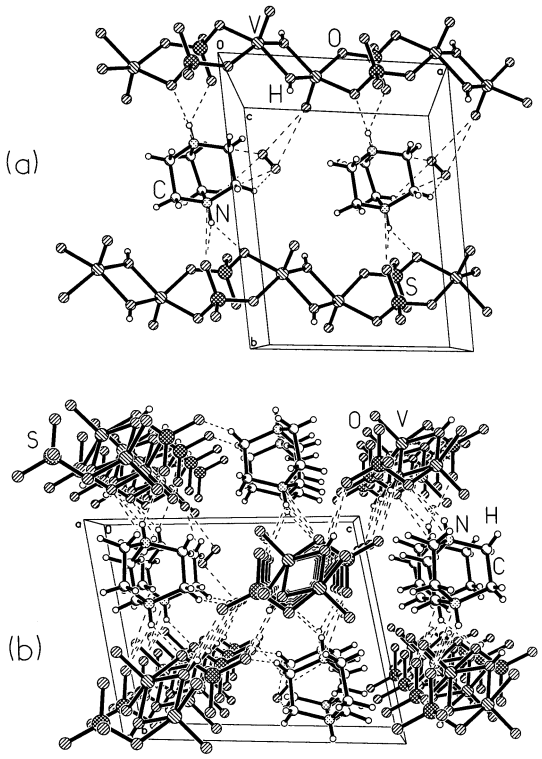

Figure 2. (a) Structure of **I** in the *ab*-plane showing the interaction between the amine and the inorganic chains leading to a layerlike network. Dotted lines represent hydrogen bond interactions. (b) View down the *b*-axis showing the packing of chains in **I**.

OH group creates a {−V−(OH)−V−(OH)−V−} backbone in the linear chain of $VO_4(OH)_2$ octahedra and allows the sulfate moiety to bridge symmetrically to form a tancoite[15] type topology as shown in Figure 3b. Such a structure has been found in open-framework metal phosphates[16] as well as phosphate and sulfate minerals.[17] The 1D chains in **II** are arranged parallel to one another with the diprotonated amine molecules and water molecules residing in the interchain space to form a layerlike arrangement (Figure 4a). Such layers are stacked one over the other along the *c*-axis, to form a 3D assembly as shown in Figure 4b.

The octahedral V−O bond distances in **II** are in the range 1.960(5)−2.055(5) Å with an average V−O distance of 2.012(5) Å. The *cis*-O−V−O bond angles are between 87.6(2)° and 92.4(2)° [$(cis\text{-O}-\text{V}-\text{O})_{av}$ = 90.0°], and the *trans*-O−V−O bond angle is 180°. The tetrahedral S−O bond distances are in the range 1.427(7)−1.508(6) Å [$(\text{S}-\text{O})_{av}$ = 1.469(6) Å], and the O−S−O bond angles are in the range 106.4(4)−112.4(4)° [$(\text{O}-\text{S}-\text{O})_{av}$ = 109.44(4)°]. The V−(μ-O)−(H) distance in the [V(1)−(μ_2-OH)$_2$−V(2)] moiety, found to be in the range 1.960(5)−1.964(5) Å, is comparable to other V−(μ-O)−(H) distances reported earlier.[13] This, along with the observed electron density near the oxygen

(13) (a) Khan, M. I.; Chang, Y. D.; Chen, Q.; Salta, J.; Lee, Y. S.; O'Connor, C. J.; Zubieta, J. *Inorg. Chem.* **1994**, *33*, 6340 and references therein. (b) Khan, M. I.; Cevik, S.; Powell, D.; Li, S.; O'Connor, C. J. *Inorg. Chem.* **1998**, *37*, 81 and references therein.

(14) (a) Brese, N. E.; O'Keeffe, M. *Acta Crystallogr.* **1991**, *B47*, 192. (b) Brown, I. D.; Altermatt, D. *Acta Crystallogr.* **1985**, *B41*, 244.

(15) Hawthrone, F. C. *TMPM, Tschermaks Mineral. Petrogr. Mitt.* **1983**, *31*, 121.

(16) (a) Simon, N.; Loiseau, T.; Ferey, G. *J. Mater. Chem.* **1999**, *9*, 585. (b) Lethbridge, Z. A. D.; Lightfoot, P.; Morris, R. E.; Wrags, D. S.; Wright, P. A.; Vick, A. K.; Vaughan, G. *J. Solid State Chem.* **1999**, *142*, 455.

(17) Hawthrone, F. C.; Krivovichev, S. V.; Burns, P. C. *Rev. Mineral. Geochem.* **2000**, *40*, 1.

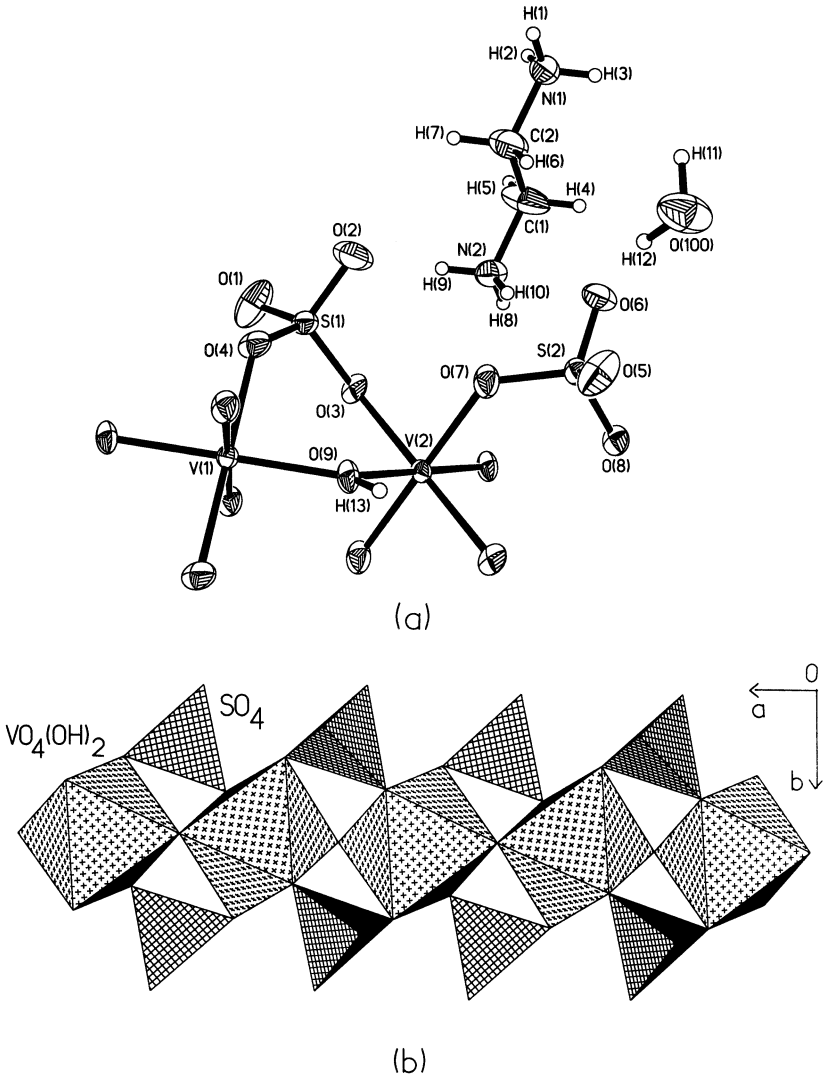

Figure 3. (a) ORTEP plot of $[H_3N(CH_2)_2NH_3][V^{III}(OH)(SO_4)_2]\cdot H_2O$, **II**. The asymmetric unit is labeled. (b) Polyhedral view of the inorganic part of **II** along the *c*-axis, showing symmetrical bridging of the sulfate tetrahedra. Note the tancoite type chain motif.

(O(9)) in the difference Fourier map and the results from the BVS calculations, leads to the identification of O(9) as that of a hydroxyl group. BVS calculations [V(1) = 2.91 and V(2) = 2.92] also indicate the valence state of V to be +3. Selected values of the bond distances and angles in **II** are listed in Table 4, and the various hydrogen bond interactions in Table 6.

$[H_2N(CH_2)_4NH_2][(V^{IV}O)(H_2O)(SO_4)_2]$, III. The asymmetric unit of **III** consists of 19 non-hydrogen atoms out of which 13 belong to the inorganic chain and 6 belong to the guest molecules (Figure 5a). The strand type structure is made up from strictly alternating $VO_5(H_2O)$ octahedra and SO_4 tetrahedra running along the *a*-axis. The vanadium octahedra are bridged by the sulfate tetrahedra in a trans fashion to form a simple 1D chain as shown in Figure 5b. The $VO_5(H_2O)$ octahedra are defined by two oxygen donors from two adjacent sulfates, two from a bidentate sulfate unit, and an oxygen from the aqua ligand besides the terminal oxide group. The vanadyl oxygen bond length (V(1)—O(1) = 1.582(2) Å) is comparable to that reported in the literature.[12] The V(1)—O(6) bond trans to the V=O group is longer (2.351(2) Å) than the remaining four V—O bonds (1.996(2)−2.046(2) Å). The S atoms form two S—O—V bonds [S(2) with each of the adjacent vanadium atoms with the S(1) atom coordinating in the equatorial cis position of V(1)], and the remaining two form S=O terminal bonds. The S—O distances in the sulfate group lie in the 1.436(2)−1.502(2) Å range, the longest bonds involving the oxygen atom coordinated to the V center. The *cis*-O—V—O bond angles are between 64.07(8)° and 105.22(12)° [(*cis*-O—V—O)$_{av}$ = 89.42(10)°], and the *trans*-O—V—O bond angles are between 156.76(11)° and 162.07(10)° [(*trans*-O—V—O)$_{av}$ = 158.63(10)°]. The O—S—O bond angles are in the range 102.54(11)−113.0(2)°, with an average of 109.41(10)°. The values of bond distances and angles indicate that both $VO_5(H_2O)$ and SO_4 polyhedra are highly distorted. BVS calculations [V = 4.11] indicate the valence state of vanadium to be +4. The 1D strands in **III** are interconnected through hydrogen bonds formed from the terminal water molecule of one chain and the oxygen of the edge-sharing sulfate tetrahedra of another chain as shown in Figure 5c. Such layers are held together by the hydrogen bond assembly formed by the diprotonated amine molecules and the framework oxygens (Figure 6). Selected values of the bond

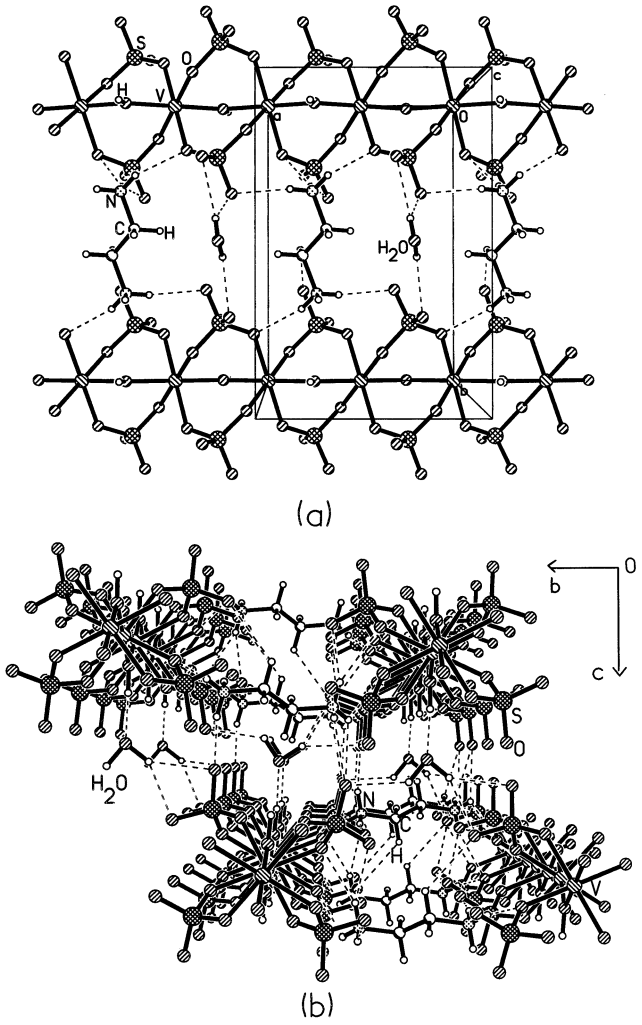

Figure 4. (a) Ball and stick view of the layers in **II**, showing the hydrogen bonded assembly. Note the extended hydrogen bonds formed by the amine and water molecules. (b) Projection of **II** along [001] showing hydrogen bond interactions between the amine, water, and the inorganic chains.

distances and angles in **III** are listed in Table 5 and the various hydrogen bond interactions in Table 6.

Thermal Behavior. TGA curves (N_2 atmosphere, range 30−900 °C, heating rate 5 °C/min) of **I**−**III** given in Figure 7 show distinct mass losses. TGA of **I** reveals the loss of guest water molecules at 100 °C [obsd = 3.7%, calcd = 4.06%], and a gradual weight loss in the 250−800 °C range corresponding to the loss of the amine, the hydroxyl group, and SO_3 [obsd = 63.26%, calcd = 63.06%]. The sample heated at 900 °C diffracts weakly, and the PXRD pattern could not be characterized. In **II**, there is a two-step weight loss corresponding to the loss of extra-framework water at 125 °C [obsd = 6.1%, calcd = 5.3%], and the major loss in the 300−550 °C range corresponds to the loss of OH, SO_3, and the amine molecule [obsd = 70.26%, calcd = 69.96%]. The PXRD pattern of the sample heated at 900 °C corresponds to V_2O_5 (JCPDS file card no. 41-1426). The TGA curve of **III** shows the loss of adsorbed water and bonded water [obsd = 10.1%, calcd = 4.93%] in the range 100−180 °C and loss of the amine along with SO_3 [obsd = 71.4%, calcd = 72.28%] in the 300−500 °C range. The PXRD pattern of the sample heated at 900 °C corresponds to VO_2 (JCPDS file card no. 44-0253).

Magnetic Properties. We studied the magnetic properties of **I**−**III** in the 4−300 K range (applied field, 5000 and 200 Oe). All the three compounds are predominantly paramagnetic as evidenced by their susceptibility versus temperature plots (Figure 8). There is no long-range ordering at various applied fields (200 and 5000 Oe). The inverse susceptibility data (Figure 8 inset) show a linear behavior at high temperatures yielding negative Curie temperatures ($\theta_p = -13$ K for **I** and −6 K for **III**), indicating weak antiferromagnetic interactions in **I** and **III**. The effective magnetic moment per vanadium atom calculated from the linear fit of the χ_M^{-1} versus T curve (range 150−300 K) is lower than expected for vanadium(IV) centers (1.48 μ_B for **I** and 1.51 μ_B for **III**, theoretical $\mu_{eff} = 1.73\ \mu_B$) and is comparable to the values reported in the literature.[18] There is a weak shoulder in the χ_M versus T plot of **I** which cannot be attributed to antiferromagnetic ordering. Compound **II** exhibits weak ferromagnetic interactions as indicated by the positive Curie temperature ($\theta_p = +24$ K). The magnetic moment per V^{3+} center is comparable with the theoretical value (3.08 μ_B for **II**, $\mu_{eff} = 2.83\ \mu_B$).

Discussion

The vanadium phosphate system is known to have a rich structural chemistry owing to the accessibility of more than one oxidation state and the ability of the vanadium−oxygen polyhedra and phosphate tetrahedra to form a variety of frameworks with interesting properties.[19] The present study of vanadium sulfates expands the family of organically templated sulfate based materials.[5,6] The vanadium sulfates contain vanadium in oxidation state less than +5. The only such vanadium sulfates known to us are the inorganic−organic hybrid materials described by Khan et al.[13,20] and those found in the molten gas system $M_2S_2O_7-V_2O_5/SO_2-O_2-SO_3-N_2$ (M = Na, K or Cs), involved in the production of sulfuric acid.[21] A series of vanadium jarosites has been reported recently.[22]

There are many noteworthy features in the chain structures of **I**−**III**. Thus, **I** represents the first square-pyramidal/tetrahedral (SP/T) chain in the metal−sulfate family. Each tetravalent vanadium atom in the inorganic chain of **I** is coordinated by five oxygen atoms in a square-pyramidal arrangement with one short V=O distance characteristic of a vanadyl group. Two VO_5 pyramids share a common edge

(18) (a) Hung, L.-I.; Wang, S.-L.; Kao, H.-M.; Lii, K.-H. *Inorg. Chem.* **2002**, *41*, 3929. (b) Tsai, Y.-M.; Wang, S.-L.; Huang, C.-H.; Lii, K.-H. *Inorg. Chem.* **1999**, *38*, 4183. (c) Do, J.; Zheng, L.-M.; Bontchev, R. P.; Jacobson, A. J. *Solid State Sci.* **2000**, *2*, 343. (d) Boudin, S.; Guesdon, A.; Leclaire, A.; Borel, M.-M. *Int. J. Inorg. Mater.* **2000**, *2*, 561.

(19) Fernandez, S.; Mesa, J. L.; Pizarro, J. L.; Lezama, L.; Arriortua, M. I.; Rojo, T. *Chem. Mater.* **2002**, *14*, 2300 and references therein.

(20) Khan, M. I.; Cevik, S.; Doedens, R. J. *Chem. Commun.* **2001**, 1930 and references therein.

(21) Nielsen, K.; Fehrmann, R.; Eriksen, K. M. *Inorg. Chem.* **1993**, *32*, 4825.

(22) (a) Grohol, D.; Papoutsakis, D.; Nocera, D. G. *Angew. Chem., Int. Ed.* **2001**, *40*, 1519. (b) Papoutsakis, D.; Grohol, D.; Nocera, D. G. *J. Am. Chem. Soc.* **2002**, *124*, 2647. (c) Grohol, D.; Nocera, D. G. *J. Am. Chem. Soc.* **2002**, *124*, 2640.

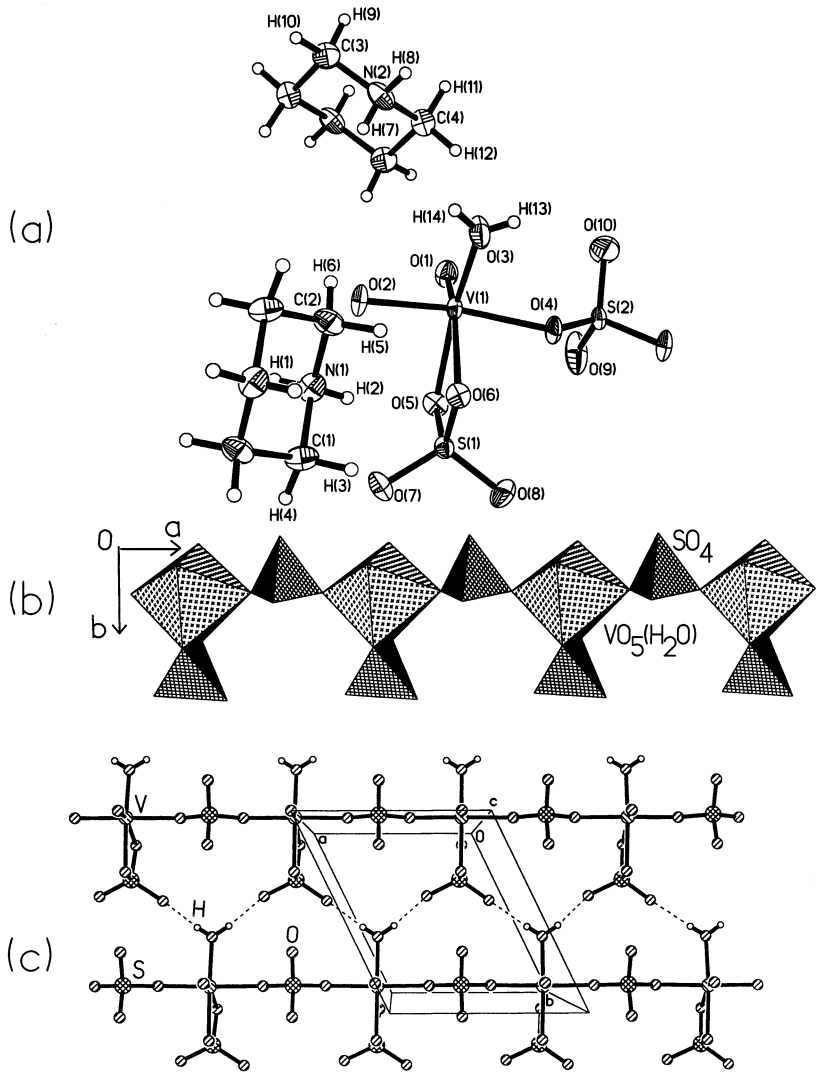

Figure 5. (a) ORTEP plot of $[H_2N(CH_2)_4NH_2][(V^{IV}O)(H_2O)(SO_4)_2]$, **III**. The asymmetric unit is labeled. (a) Polyhedral view of the inorganic part of **III**, along the *c*-axis showing the strict alternation of the sulfate tetrahedron and the vanadium octahedron. (c) Structure of **III** in the *ab*-plane. Note the interactions between the inorganic chains. Dotted lines represent hydrogen bond interactions.

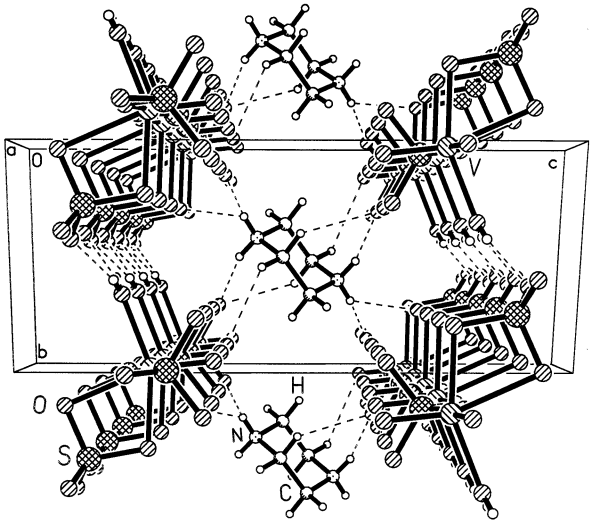

Figure 6. 3D assembly formed by the chains and the amine molecules in **III**, creating channels.

to form V_2O_8 dimers with trans orientation of V=O units in each dimer to minimize nonbonded oxygen−oxygen repulsion.[23] The five-coordinated vanadium exhibiting square-pyramidal geometry is not unique to **I** and has been observed in $V/O/PO_4$ systems,[24] but they generally possess 2D and 3D structures with more than one polyhedral form for the V center. The structure of **I** can be related to the structure of the mineral kröhnkite,[17] with alternating CuO_6 and SO_4 units forming four-membered rings, corner-linked to give 1D chains. In **I**, the CuO_6 octahedra are replaced by the V square-pyramid dimer as shown in Figure 9a. The kröhnkite chain topology with tetrahedral atoms has been observed in open-framework Co, Ga, and Al phosphates.[25]

The topology of **II** (Figure 9b) occurs in some sulfate minerals[17] besides a few other open-framework solids. Thus,

(23) (a) Bontchev, R. P.; Do, J.; Jacobson, A. J. *Angew. Chem., Int. Ed.* **1999**, *38*, 1937. (b) Do, J.; Zheng, L.-M.; Bontchev, R. P.; Jacobson, A. J. *Solid State Sci.* **2000**, *2*, 343.
(24) Soghomonian, V.; Haushalter, R. C.; Chen, Q.; Zubieta, J. *Inorg. Chem.* **1994**, *33*, 1700.
(25) (a) Chippindale, A. M.; Tuner, C. *J. Solid State Chem.* **1997**, *128*, 318. (b) Choudhury, A.; Natarajan, S.; Rao, C. N. R. *J. Chem. Soc., Dalton Trans.* **2000**, 2595 and references therein. (c) Loiseau, T.; Serpaggi, F.; Ferey, G. *Chem. Commun.* **1997**, 1093.

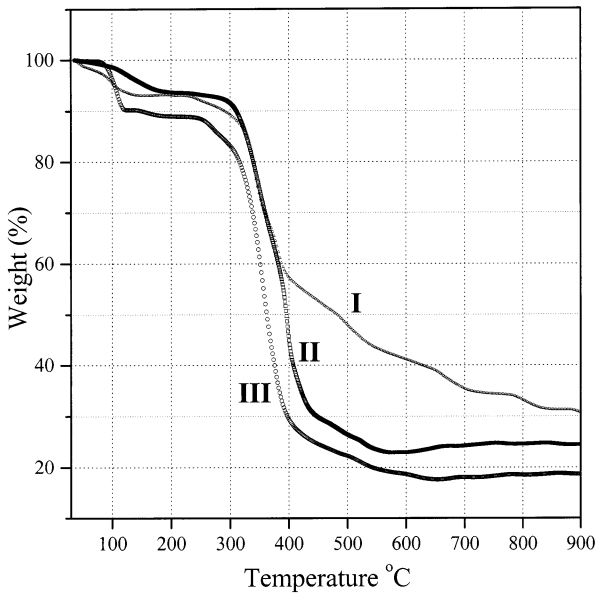

Figure 7. TGA curves of compounds **I**−**III**.

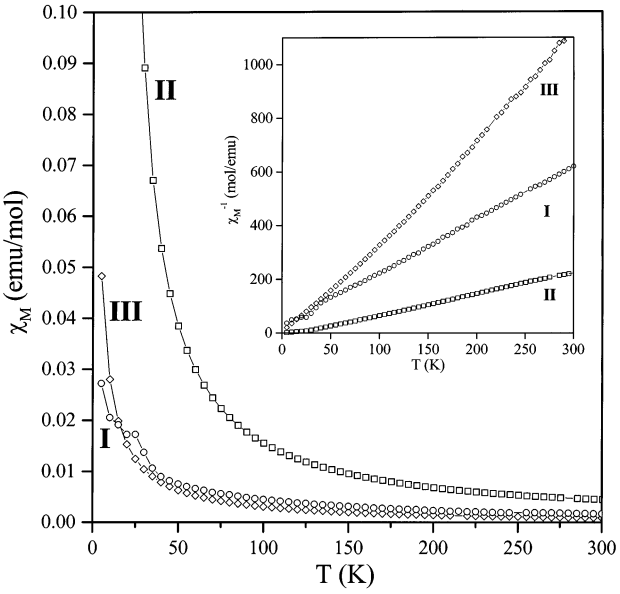

Figure 8. Temperature variation of the magnetic susceptibility (at 5000 Oe) for compounds **I**−**III**. Inset shows the temperature variation of χ_M^{-1} for **I**−**III**.

the structure of the minerals sideronatrite, metasideronatrite, and tancoite are based on this topology. The variants of the tancoite chain have been encountered in phosphate-based minerals of Al,[26] Ga,[27] and also Fe.[28] Furthermore, synthetic 2D and 3D phosphates possessing the tancoite type chain motif are known, and the chain structure is reported to transform to 2D and 3D structures in gallium phosphate systems.[27,29] We have recently obtained a 1D vanadium sulfate, templated by DABCO, $[HN(CH_2)_6NH][V^{III}(OH)(SO_4)_2]\cdot H_2O$, **IV**, with a topology related to the tancoite. In **IV**, the $VO_4(OH)_2$ octahedra share their vertices in an alternating cis−trans fashion in contrast to **II**, where the octahedra are trans connected. The formula of **IV** is same as **II**, the only difference being in the templating amine. The unit cell parameters in **IV** are $a = 18.6664$ Å, $b = 12.0098$ Å, $c = 12.4810$ Å, $\alpha = 90.000°$, $\beta = 108.441°$, $\gamma = 90.000°$, $Z = 8$, and $V = 2654.31$ Å^3.

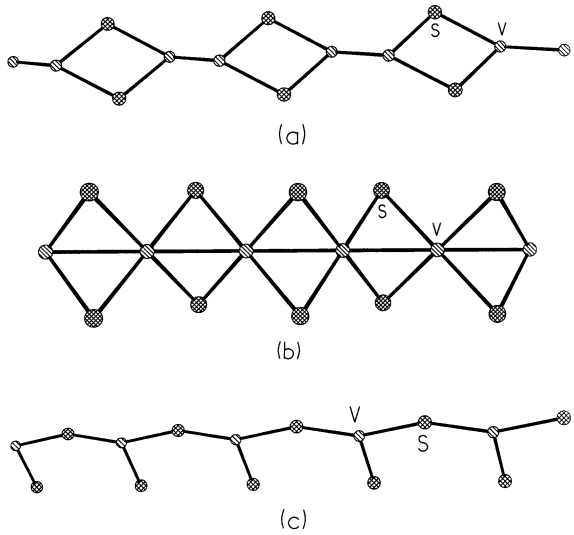

Figure 9. T-atom (V, S) connectivities in **I**−**III**.

The structure of **III** is based on the backbone formed by the strict alternation of corner-sharing vanadium octahedra and SO_4 tetrahedra as shown in Figure 9c.

The $[M(TO_4)\Phi_4]$ chain backbone in **III** is the simplest 1D structure and forms the basic motif in the mineral group chalcabthite.[17] Even though the edge-sharing interactions between vanadium octahedra and sulfate tetrahedra in **III** are not unique, this rare connectivity expands the structural possibilities for such materials. A similar single stranded structure formed by vanadium sulfate is reported in the literature.[30] It is noteworthy that the magnetic properties are sensitive to the structural topology of the linear chains. While the sulfate chains formed by the V^{4+} ions show antiferromagnetic interactions, the chain made up of V^{3+} centers shows ferromagnetic interactions. Further studies are required to fully understand the relations between magnetic behavior and structural topology.

The new 1D chains reported here provide another illustrative case of the templating effect of organic amines on oxide type frameworks. With the variation of templating agent and crystallization conditions, new compounds with novel structural features are obtainable. A noticeable reduction at the metal center occurs during the synthesis of **I** and **II**. The reducing agent may possibly be the amine or the alcohol solvent.[31] Since the metal source in **II** and **III** is the same and no reduction occurs at the metal center in **III** where water

(26) (a) Attfield, M. P.; Morris, R. E.; Burshtin, I.; Campana, C. F.; Cheetham, A. K. *J. Solid State Chem.* **1995**, *118*, 412. (b) Lii, K. H.; Wang, S. L. *J. Solid State Chem.* **1997**, *128*, 21.
(27) (a) Lin, H. M.; Lii, K. H. *Inorg. Chem.* **1998**, *37*, 4220. (b) Walton, R. I.; Millange, F.; O'Hare, D.; Paulet, C.; Loiseau, T.; Ferey, G. *Chem. Mater.* **2000**, *12*, 1979. (c) Walton, R. I.; Millange, F.; Le Bail, A.; Loiseau, T.; Serre, C.; O'Hare, D.; Ferey, G. *Chem. Commun.* **2000**, 203. (d) Bonhomme, F.; Thoma, S. G.; Nenoff, T. M. *J. Mater. Chem.* **2001**, *11*, 2559.
(28) (a) Cavellec, M.; Riou, D.; Greneche, J. M.; Ferey, G. *Inorg. Chem.* **1997**, *36*, 2187. (b) Choudhury, A.; Rao, C. N. R. *Zh. Strukt. Khim.* **2002**, *43*, 681. (c) Mahesh, S.; Green, M. A.; Natarajan, S. *J. Solid State Chem.* **2002**, *165*, 334.
(29) Livage, C.; Millange, F.; Walton, R. I.; Loiseau, T.; Simon, N.; O'Hare, D.; Ferey, G. *Chem. Commun.* **2001**, 994.
(30) Richter, K. L.; Mattes, R. *Inorg. Chem.* **1991**, *30*, 4367.

was used as the solvent, it would appear that the alcohol solvent might play a role in the reduction process. This aspect however, needs to be investigated further.

(31) Warren, C. J.; Haushalter, R. C.; Rose, D. J.; Zubieta, J. *Chem. Mater*. **1997**, *9*, 2694.

Supporting Information Available: X-ray crystallographic information in CIF format for the structure determination of **I**−**IV**. This material is available free of charge via the Internet at http://pubs.acs.org.

IC020645V